ACS OMEGA

http://pubs.acs.org/journal/acsodf

Review

Recent Developments of Electrospinning-Based Photocatalysts in Degradation of Organic Pollutants: Principles and Strategies

Morasae Samadi* and Alireza Zaker Moshfegh*

Cite This: *ACS Omega* 2022, 7, 45867−45881

Read Online

ACCESS | Metrics & More | Article Recommendations

ABSTRACT: Electrospinning is a simple and cheap process for forming one-dimensional (1D) nanofibers with controllable size, morphology, and chemistry. Besides these, the ultrahigh surface area with industrialization capability has attracted extensive interest in the research community. On the other hand, a photocatalytic process is a promising method for degrading organic pollutants that cannot be removed by conventional wastewater treatment. This review focuses on the recent progress of electrospun nanofibers for the photocatalytic degradation of water pollutants. The linkage between the electrospinning technique and the photocatalytic process is classified into two main categories: (1) polymeric electrospun nanofibers as a sacrificed template to form 1D photocatalysts and (2) polymeric electrospun nanofibers as a carrier of photocatalyst materials. We have thoroughly discussed the principles and fundamental issues of electrospinning as well as two main strategies to design and fabricate nanofiber-based photocatalysts for the ideal photodegradation of organics pollutants. The results of data mapping using VOSviewer demonstrated the recent trend and the importance of this field among researchers and engineers. Moreover, we have elaborated on the limitations and potential benefits of the two categories of electrospinning-based photocatalyst fabrication and practical application that will open new directions for future research.

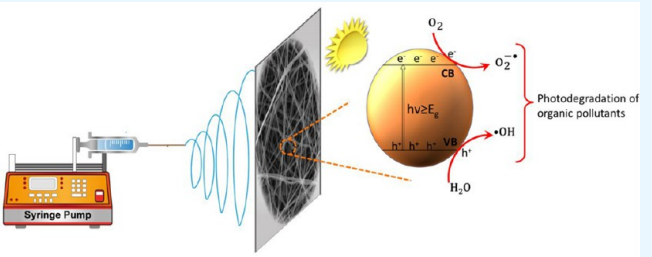

1. INTRODUCTION

Although 71% of the earth is covered by water, only 1% can be used as drinking water by humans. Increasing industrial activities and world population growth have resulted in the discharges of anthropogenic and industrial pollutants in water streams. Some of these pollutants cannot be removed by applying conventional wastewater treatment plants and thus create environmental crises. Some organic substances, such as pharmaceutical products, organic dyes, and pesticides, are included in this category. The development of advanced oxidation processes (AOPs) promises efficient purification to remove about 100% of these substances. In AOPs, strong oxidants such as $^{\bullet}OH$, H_2O_2, and $O_2^{-\bullet}$ are generated, which can effectively decompose organic pollutants. Among AOPs, photocatalytic remediation is encouraging due to its low cost and complete mineralization of organic pollutants.[1,2]

Nanomaterials possess a large surface-to-volume (A/V) ratio, which make them good candidates for catalytic and photocatalytic activity. The advantages of applying photocatalysts for water purification are their low cost, environmental friendliness, reusability, and simplicity. Also, in contrast to the conventional wastewater treatment methods, no secondary pollutions are generated.[3] In the photocatalytic process, a semiconductor is excited by light illumination and charge carriers, namely, electron (e^-) and hole (h^+), are generated in the conduction band (CB) and valence band (VB), respectively. Recombination of electron−hole pairs should be prevented to use these photogenerated charge carriers in chemical redox reactions. Currently, different strategies are utilized to satisfy this challenge. Also, another demand in the photocatalytic process is investigating the possibility of using natural sunlight instead of artificial light as an exciting light source due to a fossil fuel shortage and climate change. Solar light, abundant and clean energy, consists of 4% ultraviolet (UV) rays, 43% visible light, and 53% infrared (IR) radiation. Therefore, designing semiconductors activated by visible light is more appealing to meet maximum efficiency under solar light.[4] Different approaches for enhancing the efficiency of semiconductor photocatalysts and designing their structures are discussed in section 3.

Since photocatalysts are very effective in environmental remediation, many synthesis methods have been used to achieve their diversity. Utilizing electrospinning with the potential of large-scale and industrialized production can be promising for

Received: August 31, 2022
Accepted: November 2, 2022
Published: December 9, 2022

fabricating photocatalysts for wastewater purification. It is well established that a nanofiber photocatalyst is much more efficient than its nanoparticle analog for photocatalytic applications.[5] Electrospinning is a simple, versatile, and cheap method for fabricating various 1D nanofibers with different applications. The final nature of these nanowoven nanofibers makes them a good candidate for application as a membrane filter. Also, their high surface area enhances the adsorption capacity for pollutant removal in wastewater.[6,7] Different techniques, such as modifying the polymer composition, engineering the chemical surface structure, and immobilizing active and functionalized species, can improve the ability of the electrospun nanofiber membrane in wastewater treatment.[8] Besides, a nanofiber photocatalyst is much more efficient than its nanoparticle analog for photocatalytic application.[5]

This review systematically divided all of the research in this field into two main categories to establish a foundation and application for readers. First, it considers the role of electrospun nanofibers as a template for photocatalyst formation, and second, it reflects on the electrospun fibrous membrane for photocatalyst immobilization. Due to the versatility and tunability for the fabrication of different electrospinning-based photocatalysts, various reviews have been published in recent years.[9−11] Some of them have been devoted to studying the role of electrospun membranes in the immobilization of a photocatalyst,[9] and others have addressed pure electrospun photocatalysts in which a polymer act as a sacrificial agent.[10] We address both aspects and summarize recent advances in photocatalyst design. To the best of our knowledge, there is no published article that reviews different electrospun photocatalysts applied in the water purification process. Furthermore, we use the VOSviewer software to analyze this field's intellectual process and temporal changes to present a historical perspective. We provide an overview of different photocatalysts prepared by electrospinning for water purification and provide a detailed analysis of these materials. Also, the challenges and opportunities are discussed for future research directions.

2. ELECTROSPINNING TECHNIQUE

Electrospinning is an effective method to fabricate 1D nanofibers from organic, inorganic, and hybrid materials. Although this method was patented by Anton Formhals in 1934, with the efforts of Reneker's group to understand its complexity and theory, this technique has been given more attention. The schematic in Figure 1 shows a basic setup for the electrospinning method, including a high-voltage supply, a polymer solution filled in a syringe (spinneret), and a collector placed at a certain distance away from the syringe tip. Organic polymers are commonly filled in a syringe as a spinnable mixture, a uniform and homogeneous solution for electrospinning. Researchers have successfully produced nanofibers from 100 different natural and synthetic polymers with a high molecular weight.[7] The principle behind the electrospinning process is explained in the following.

The mechanical force induced by the syringe pump produces streams of droplets, which become highly charged due to applying an electrostatic potential in the range of 5−30 kV by a power supply. This electrostatic charge deforms the droplet into a cone shape, which is called a Taylor cone, as depicted in Figure 1 (inset). When the electrostatic field overcomes the viscoelastic force and surface tension at a specific applied voltage (V_c), a single jet of the charged polymer solution ejects from the apex of the Taylor cone. The jet accelerates and extends toward the collector with the opposite electric field. First, it travels straight for a particular length, which is called the stability zone, straight segment, or linear jet. Second, the jet starts to bend due to the charge repulsion and forms helical loops called whipping jets or an instability zone. Finally, jet elongation occurs and it solidifies as nanofibers on a collector by solvent evaporation.[12] The diameter of the terminal jet (d_t), which represents the diameter of the final nanofiber, is expressed by the following equation[7]

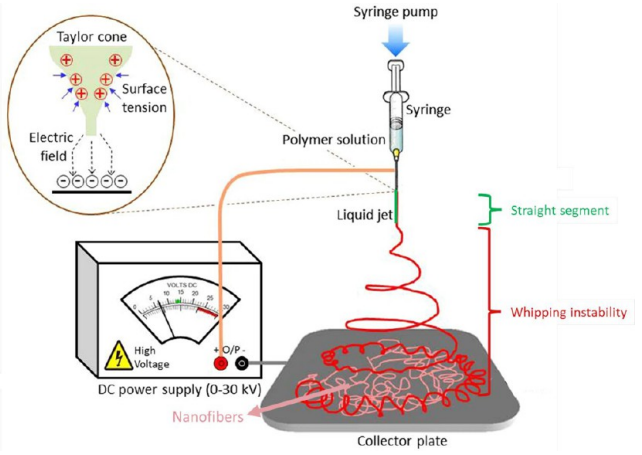

Figure 1. Schematic of the electrospinning technique for the formation of nanofibers. Reproduced with permission from ref 15. Copyright 2018 Springer Nature.

$$d_t = \left(\gamma\varepsilon\frac{Q^2 2}{I^2\pi(2\ln\chi - 3)}\right)^{1/3} \quad (1)$$

where γ is the surface tension of the solution, ε is the dielectric constant of the surrounding medium of the jet, Q is the flow rate of the liquid, I is the electric current through the jet, and χ corresponds to the dimensionless wavelength of the bending instability, which is correlated to the radius of the bending perturbation divided by the radius of the jet.[7]

Different parameters such as (1) polymer solution variables (concentration, viscosity, conductivity, polymer molecular weight, and solvent vapor pressure), (2) ambient conditions (temperature and humidity), and (3) operational conditions (applied voltage, syringe tip to collector distance, polymer feeding rate, and collector type) can cause the production of nanofibers with different structures. Taylor developed a theoretical simulation to determine the effects of the main parameters in electrospinning.[13] Equation 2 expresses the relationship between the critical voltage (V_c) for polymer jet formation and other operation parameters[12]

$$V_c^2 = \frac{4H^2}{L^2}\left(\ln\frac{2L}{R} - \frac{3}{2}\right)(1.30\pi\gamma R)(0.09) \quad (2)$$

where γ is the surface tension of the spinning solution, L is the needle length, R is the needle radius, and H is the distance from the needle tip to the collector. In general, there is a complex interaction between all of the parameters, and some of them have two opposite impacts on the fibers' quality; therefore, these parameters should be carefully optimized to achieve the desired results. Uniform, beadles, and thin nanofibers with high surface area are encouraging for application in photocatalytic processes. One of the main factors for fiber uniformity is solidifying and drying the as-deposited fiber on the collector. On the basis of

https://doi.org/10.1021/acsomega.2c05624
ACS Omega 2022, 7, 45867−45881

Table 1. Effect of Different Electrospinning Parameters on the Final Nanofibers' Properties

parameters	effects on the final nanofibers' properties
polymer solution parameters	
solvent vapor pressure	very high volatility causes immediate solidification of the polymer jet upon exiting from the spinneret and blocks the syringe tip
	very low volatility results in the deposition of wet fibers on a collector
solvent dielectric constant	increase in dielectric constant needs a higher applied voltage to achieve a stable jet
polymer molecular weight	adequate polymer chain entanglement required for uniform nanofiber formation
	low molecular weight tends to generate beads instead of fibers
solution concentration	polymer concentration affects the viscosity and surface tension of the solution
	at a particular concentration, chain entanglement occurs
	below this, polymer beads form instead of continuous fibers, and at a higher concentration, no jet forms due to high viscoelastic force
solution electrical conductivity	its high amounts deplete electrostatic repulsion and prevent Taylor cone generation for jet initiation
	completely insulating solution is difficult to electrospin due to the inability to conduct charges from inside the solution to its surface
operational conditions	
flow rate	increasing its values results in the formation of large-diameter fibers
syringe tip to collector distance	at a specific range, complete extension and solidification of the jet arise, ensuring the formation of uniform and solid fibers
	in general, as the distance increases, thinner fibers form
applied voltage	higher voltages generally favor the formation of thinner fibers
ambient conditions	
relative humidity	at suitable relative humidity, the evaporation rate of the solvent is fast enough and favors the formation of dry and thin fibers
	lowering this amount leads to quick solvent evaporation and hinders jet extension
	at very high relative humidity, water vapor replaces by evaporated solvent and induces morphological changes
ambient temperature	at elevated temperatures, the surface tension and solution viscosity are reduced, favoring thinner fiber formation
	in contrast, solvent evaporation at higher temperatures hinders adequate extension of the jet

different documents, Table 1 summarizes the influence of different parameters on the nanofibers' quality.[7,14]

Changing these variables leads to the formation of different structures, including nonwoven, porous, hollow, core−shell, helical, and Janus electrospun nanofibers. The diversity of structures causes different applications in air and water filtration, supercapacitors, batteries, catalysis, and drug delivery.[7] In this article, we focus on applying the electrospinning process to the degradation of different organic pollutants using appropriate semiconductor photocatalysts.

3. PHOTOCATALYTIC PROCESS

Figure 2 illustrates the degradation of organic pollutants through a heterogeneous photocatalysis process. Illuminated light with

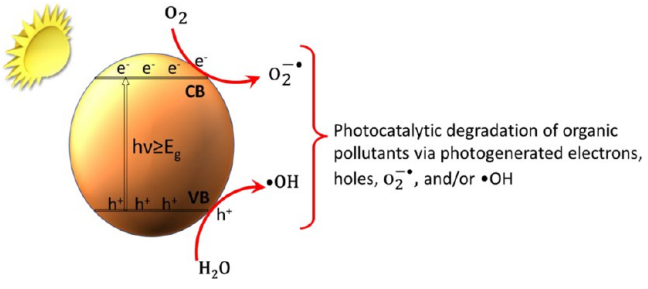

Figure 2. Schematic of the generation of charge carriers and reactive oxygen species (ROS) during a photocatalytic process.

an energy $h\nu$ of more than the semiconductor band gap (E_g) excites the electrons (e^-) to the conduction band (CB), and holes (h^+) remain in its valence band (VB). These electron−hole pairs as charge carriers migrate to the photocatalyst surface and conduct reduction and oxidation reactions. Meanwhile, recombining these charge carriers can lead to decreased photocatalytic efficiency. Figure 3 shows the energy levels of different semiconductors' CBs and VBs. If the generated electrons in the CB have a more negative potential than $O_2/O_2^{-\bullet}$ (−0.33 V vs NHE), the superoxide radicals ($O_2^{-\bullet}$) form which are highly active in reducing organic pollutants. Moreover, the more positive potential of the generated holes than $^\bullet OH/H_2O$ (+2.53 V vs NHE) leads to the formation of highly reactive hydroxyl radicals ($^\bullet OH$). All of these surface species formed in a semiconductor under light illumination are called reactive oxygen species (ROS). Therefore, choosing an appropriate semiconductor by considering its CB and VB energy levels can improve this process's efficiency.[2] It is well accepted that the electron, hole, $O_2^{-\bullet}$, and/or $^\bullet OH$ can control the photocatalytic pathway.[2] Therefore, understanding the nature and role of each charge carrier can determine the reaction mechanism.

To quantify a photocatalytic reaction rate, a suitable kinetic model must be applied depending on the concentrations of the reactants. At low initial concentrations of pollutants, the kinetics of the photocatalytic degradation obeys the Langmuir−Hinshelwood apparent first-order kinetics model according to the following equation[17]

$$r = \frac{dC}{dt} = \frac{kKC}{1 + KC} \tag{3}$$

where r is the rate of photodegradation (mg/L·min), C is the pollutant concentration (mg/L), t is the reaction time under light irradiation, k is the reaction rate constant (mg/L·min), and K is the pollutant adsorption coefficient (L/mg). In the case of a low initial concentration (C_0) of pollutants (C_0 = 10 mg/L), eq 3 is simplified to an apparent first-order model[17]

$$\ln\left(\frac{C_0}{C}\right) = kKt = k_{app}t \tag{4}$$

where k_{app} is the apparent first-order rate constant (min^{-1}) and can be determined as the slope of the graph of $\ln(C_0/C)$ vs the reaction time. Many researchers use various approaches to increase the quantity of k_{app}, which enhances the photocatalytic efficiency and improves the reaction yield. In this context,

https://doi.org/10.1021/acsomega.2c05624
ACS Omega 2022, 7, 45867−45881

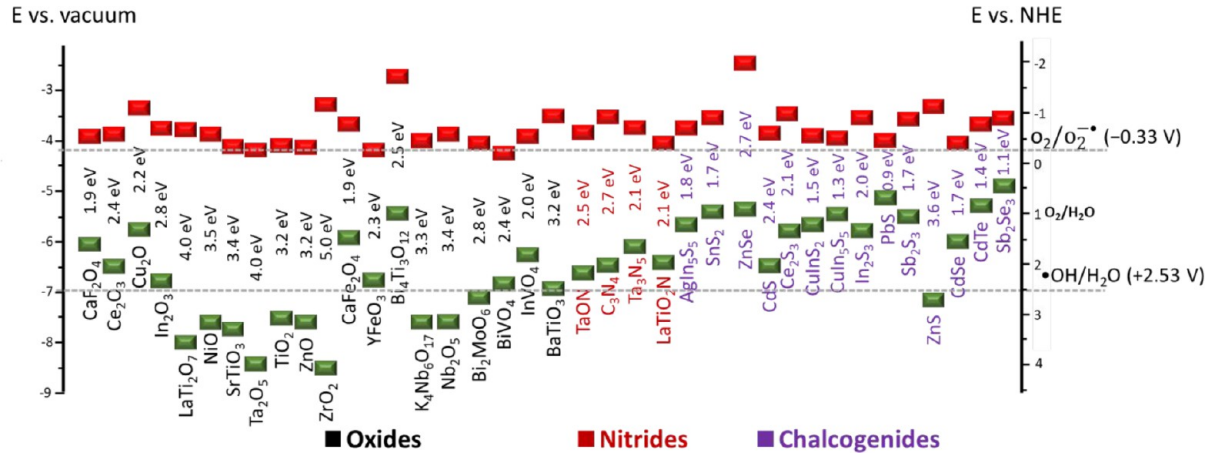

Figure 3. Band-gap energies and CB (red) and VB (green) band edge positions of the selected oxides, nitrides, and chalcogenides concerning the standard redox potentials of $O_2^{-\bullet}$ and $^\bullet OH$ generation. Reproduced with permission from ref 16. Copyright 2017 Royal Society of Chemistry.

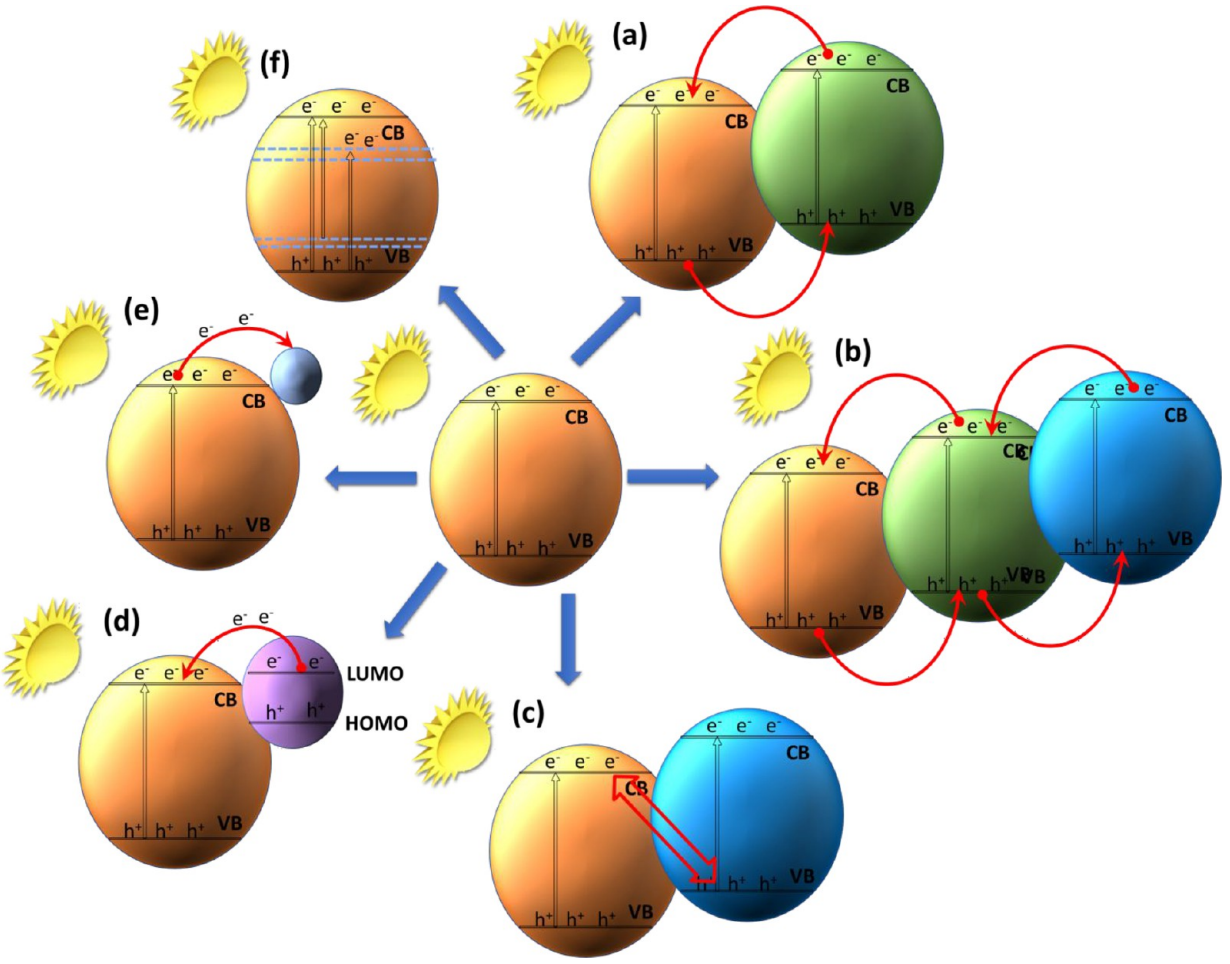

Figure 4. Schematic illustration of the formation of charge carriers (e^- and h^+) and separation on the photocatalytic surface. (a) Type II semiconductor−semiconductor heterostructures. (b) Cascade heterojunction system. (c) Z-scheme semiconductor−semiconductor heterostructures. (d) Immobilization of photosensitizers on the semiconductor surface. (e) Photoelectron trapping agent on the semiconductor surface. f) Doping or defect inducing impurity levels in the semiconductor band gap.

increasing the separation efficiency of photogenerated electron−hole pairs is the most crucial way to maximize the charge carriers generation for photocatalytic degradation.

In general, understanding the mechanism of a photocatalytic reaction can be helpful in designing an appropriate semiconductor photocatalyst by predicting the charge carriers' pathway. Figure 4 shows schematically different strategies for generating and separating electron−hole pairs. The ideal photocatalyst has a wide range of sunlight absorption, rapid migration of electron−hole pairs to the photocatalyst surface, and suitable CB and VB redox potentials for $O_2^{-\bullet}$ and $^\bullet OH$ formation. In Figure 4a, the positions of the CB and VB of the

https://doi.org/10.1021/acsomega.2c05624
ACS Omega 2022, 7, 45867−45881

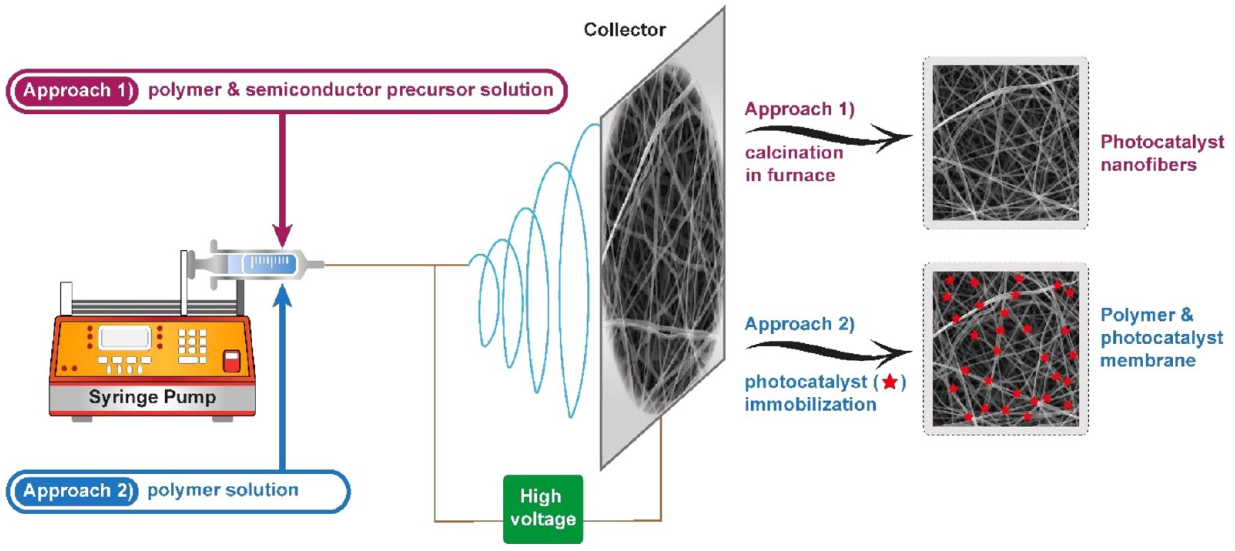

Figure 5. Overview of the fabrication process of a photocatalyst nanocomposite through the electrospinning technique.

two semiconductors relative to each other are such that photogenerated electrons and holes accumulate on two different semiconductors to enhance their separation, which is assigned to a type II heterostructure. Moreover, in Figure 4b, the cascade system for separating photogenerated electrons and holes can inhibit their recombination and favors the photocatalytic process. Figure 4c shows that the photogenerated holes in one semiconductor recombine with the photogenerated electrons in the other semiconductors. The accumulated electrons and holes in two different semiconductors participate in the photocatalytic process. This case is attributed to the Z-scheme mechanism. Figure 4d illustrates applying molecular photosensitizers or plasmonic materials adsorbed on a semiconductor, which can donate an excited electron into the semiconductor CB and enhance the photocatalytic efficiency. Figure 4e demonstrates the role of conductive materials such as metals, carbon nanotubes, and graphene as electron acceptors from the CB of semiconductors leading to an improvement in the electron−hole separation efficiency. Also, Figure 4f exhibits the action of defect states or doping in the semiconductor band structure. They allow absorbing light with a longer wavelength, and an optimal defect density can inhibit electron−hole recombination. All of these strategies can be considered for designing a desired photocatalyst for a particular reaction. In sections 4 and 5, different examples of materials fabricated by the electrospinning method to promote the separation efficiency of photogenerated electrons and holes will be reviewed.

4. PHOTOCATALYST FABRICATION BY ELECTROSPINNING

Due to the importance of 1D nanomaterials with a high aspect ratio and the ability for retardation in electron−hole recombination, electrospinning is considered an effective method to synthesize nanofiber-based photocatalysts. On the basis of the published documents, we divided the electrospinning-based photocatalysts into two main groups. Figure 5 shows an overview of these approaches. One strategy is to utilize the 1D electrospun nanofibers as a scarifying template for photocatalyst formation. In this method, the polymeric electrospun nanofibers are mainly decomposed via annealing, and semiconductor precursors are converted to the crystal structure. In the other approach, the electrospun polymeric mat is used to grow and form a semiconductor photocatalyst.

4.1. Literature Overview. On the basis of a Scopus database search and using VOSviewer data visualization and trend analysis for the research articles, as many as 1603 documents were published from 2003 (the first published article in this field) to August 31, 2022. The results are illustrated in Figure 6a, demonstrating this field's growth and activity. Moreover, the occurrences of keywords as the essential index of the research hot spot were analyzed in detail. The same-meaning keywords were merged, and the meaningless keywords were deleted. The top cited 24 keywords with their frequencies are listed in Figure 6b. Accordingly, the highest frequency semiconductors prepared by the electrospinning method for photocatalytic applications were TiO_2, ZnO, carbon nitride, CdS, SiO_2, ZnS, $SrTiO_3$, CuO, AgCl, CeO_2, and MoS_2. Moreover, degradation of methylene blue, rhodamine B, and methyl orange as organic dyes, phenolic compounds, tetracycline antibiotics, and *Escherichia coli* (*E. coli*) bacteria has been reported in the published articles. Furthermore, it was found that polyacrylonitrile (PAN), polyvinylpyrrolidone (PVP), cellulose, poly(vinyl alcohol) (PVA), and poly(vinylidene fluoride) (PVDF) are more attractive and suitable polymers.

Figure 7 provides an overlay visualization of the recent publications on electrospinning-based photocatalysts. To be more specific and focused, we have considered a set of 10 co-occurrences among the 7329 keywords using the Scopus database. Accordingly, photocatalytic degradation of pharmaceutical pollutions and pathogenic bacteria, including tetracycline antibiotics and *E. coli*, has been more interesting recently (see yellow-colored keywords in Figure 7). In addition, graphene and its derivatives have been considered in recent years; while they do not have photocatalytic properties, they can improve the separation of the photogenerated electron−hole with different mechanisms. Furthermore, with the increased

https://doi.org/10.1021/acsomega.2c05624
ACS Omega 2022, 7, 45867−45881

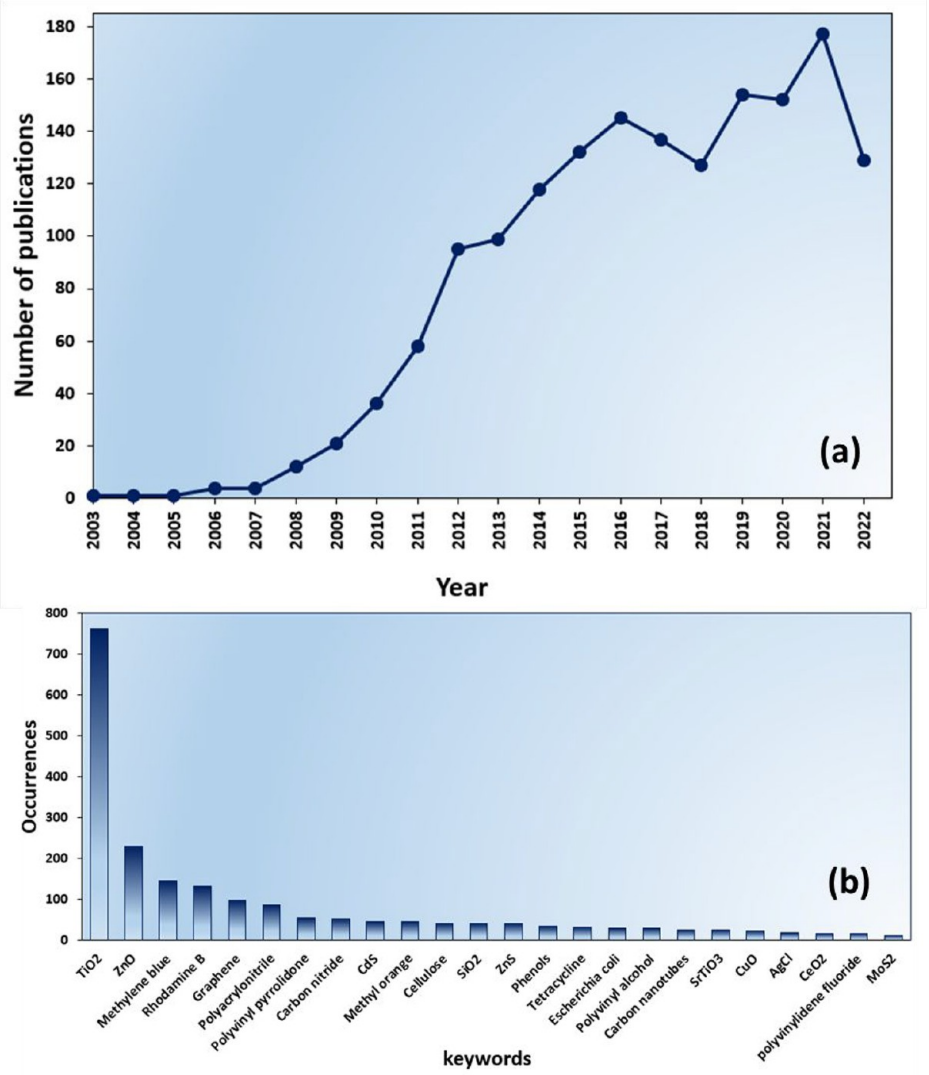

Figure 6. Statistics from the Scopus database for (a) trend of publication and (b) co-occurrence of keywords with search string (TITLE ("photocatal*") AND TITLE-ABS-KEY (electrospinning) OR TITLE-ABS-KEY (electrospun)) from 2003 to Aug 31, 2022.

knowledge about 2D materials, the application of MoS_2 and carbon nitride in photocatalytic systems has also been increased.

In addition, doping metal and nonmetal elements in semiconductors can induce their visible light activity to enhance the photocatalytic activity under solar light. Therefore, the doping process has been an attractive and focused on trend among researchers very recently. The other field of interest is the anchoring and immobilization of photocatalysts on the nanofibrous electrospun membrane, enhancing the reusability and recyclability of photocatalysts. Moreover, all of the related articles were compiled for the photodegradation of organic pollutants using the VOSviewer software (from 2003 to August 31, 2022) by applying co-occurrence of relevant keywords. Table 2 shows different chemicals and organic substances which have been mineralized or degraded by electrospinning-based photocatalysts.

4.2. Two Strategies in Preparing Photocatalysts Using Electrospinning. Before elaborating on photocatalyst preparation using the electrospinning method, the advantages of electrospinning-based photocatalysts are presented briefly based on published articles. According to this literature survey, electrospun nanofibers possess at least five advantages, including the following. (1) In contrast to the powder-type photocatalysts in the slurry system, which can be agglomerated during successive utilization, anchoring the photocatalyst on an electrospun mat leads to its stability improvement.[18,19] (2) A simple separation of free-standing photocatalyst film as a floating water treatment system facilitates its practical applications.[18,20] (3) The large surface area of the electrospun nanofibers promotes the adsorption of the organic pollutants and enhances the photodegradation efficiency.[21,22] (4) Functionalization of different chemical groups on polymeric electrospun nanofibers can boost the adsorption ability for water treatment.[21,23] (5) One-dimensional photocatalyst nanofibers can facilitate quick charge transfer due to their long axial ratio and enhance electron−hole separation for efficient photocatalytic activity.[24] All of these advantages along with the simple, affordable, and large-scale production ability make the electrospinning method a promising technique for various photocatalytic applications.[6,7]

4.2.1. Electrospun Nanofibers as a Template. The schematic for the fabrication of semiconductor photocatalyst via electrospun nanofiber template is illustrated in Figure 5 (approach 1). A suitable polymer and semiconductor precursor solution are mixed and put into the syringe to fabricate the

https://doi.org/10.1021/acsomega.2c05624
ACS Omega 2022, 7, 45867−45881

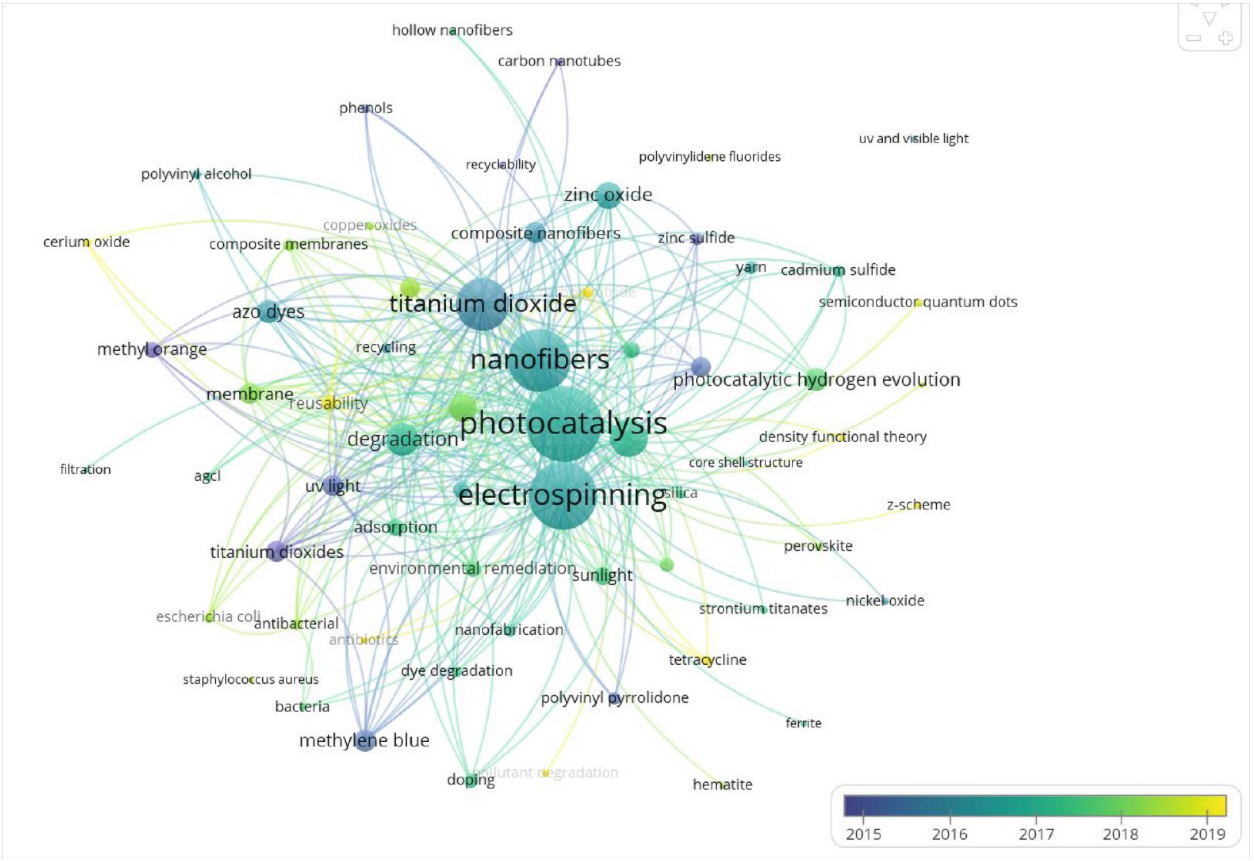

Figure 7. Overlay visualization of the electrospinning-based photocatalyst topic using VOSviewer among 7329 keywords with a threshold of at least 10 co-occurrences (Scopus database: Aug 31, 2022).

Table 2. Co-occurrence Keywords for Different Organic Pollutants Degradation by Electrospun Nanofibers

organic pollutants	number of co-occurrences
methylene blue	123
rhodamine B	111
methyl orange	45
tetracycline	16
tetracycline hydrochloride	11
4,4′-isopropylidenediphenol(bisphenol A)	10
Congo red	8
chlorophenol	8
4-nitrophenol	7
fuchsin	3
cimetidine	3
ibuprofen	3

polymer and saline precursor nanofibers. Then, the polymer was removed at high temperatures (mainly at >350 °C in air), and a semiconductor with a 1D crystal structure formed concurrently. The following research considering this method to prepare pure 1D photocatalysts is reviewed.

PVA and zinc acetate dihydrate ($Zn(CH_3COO)_2{\cdot}2H_2O$) were used to prepare an electrospinnable solution.[25] Figure 8a shows the field emission scanning electron microscopy (FESEM) image of the PVA/($Zn(CH_3COO)_2{\cdot}2H_2O$) nanofibers. It was found that ZnO nanofibers formed after calcination of these nanofibers at 460 °C. Figure 8b illustrates the FESEM of ZnO nanofibers. Calcination causes the elimination of organic substances and the crystallization of ZnO. Therefore, the size of the nanofibers is reduced upon calcination as evidenced by comparing Figure 8a and 8b.

Moreover, multiwall carbon nanotubes (MWCNTs) were added to the electrospinnable solution of the PVA/($Zn(CH_3COO)_2{\cdot}2H_2O$) to prepare a ZnO−MWCNT nanocomposite after calcination. As depicted in Figure 8c, due to the electrical conductivity of MWCNTs, the photogenerated electrons on ZnO could transfer to MWCNTs, and efficient electron−hole separation occurred. This mechanism is illustrated in Figure 4e. Moreover, thermal gravimetric analysis and differential thermal analysis (TGA-DTA) were utilized to determine the suitable temperature for polymer removal and ZnO formation. Figure 8d shows that at a temperature above 460 °C, organic substances, including PVA and an acetate group, are completely removed, and this temperature was selected for calcination. After polymer removal, the nanofiber sizes significantly decreased.

To achieve the best performance in nanocomposites containing more than one semiconductor, the weight percent of each component should be optimized. In electrospun ZnO/x wt % CuO (x = 50, 10, 5, 2.5, 1, 0.5, 0.1, and 0) nanofibers, the optimized percentage was studied regarding the methylene blue photocatalytic degradation.[26] The related reaction rate constants concerning different CuO amounts are shown in Figure 9a. The optimized ZnO/0.5CuO photocatalyst demonstrated efficient light absorption and electron−hole separation at 0.5 wt %. The mechanism of methylene blue photodegradation on the ZnO/0.5CuO nanofibers is depicted in Figure 9b. Upon solar simulator light absorption, photogenerated electron−hole pairs on both ZnO and CuO are efficiently separated, which leads to

https://doi.org/10.1021/acsomega.2c05624
ACS Omega 2022, 7, 45867−45881

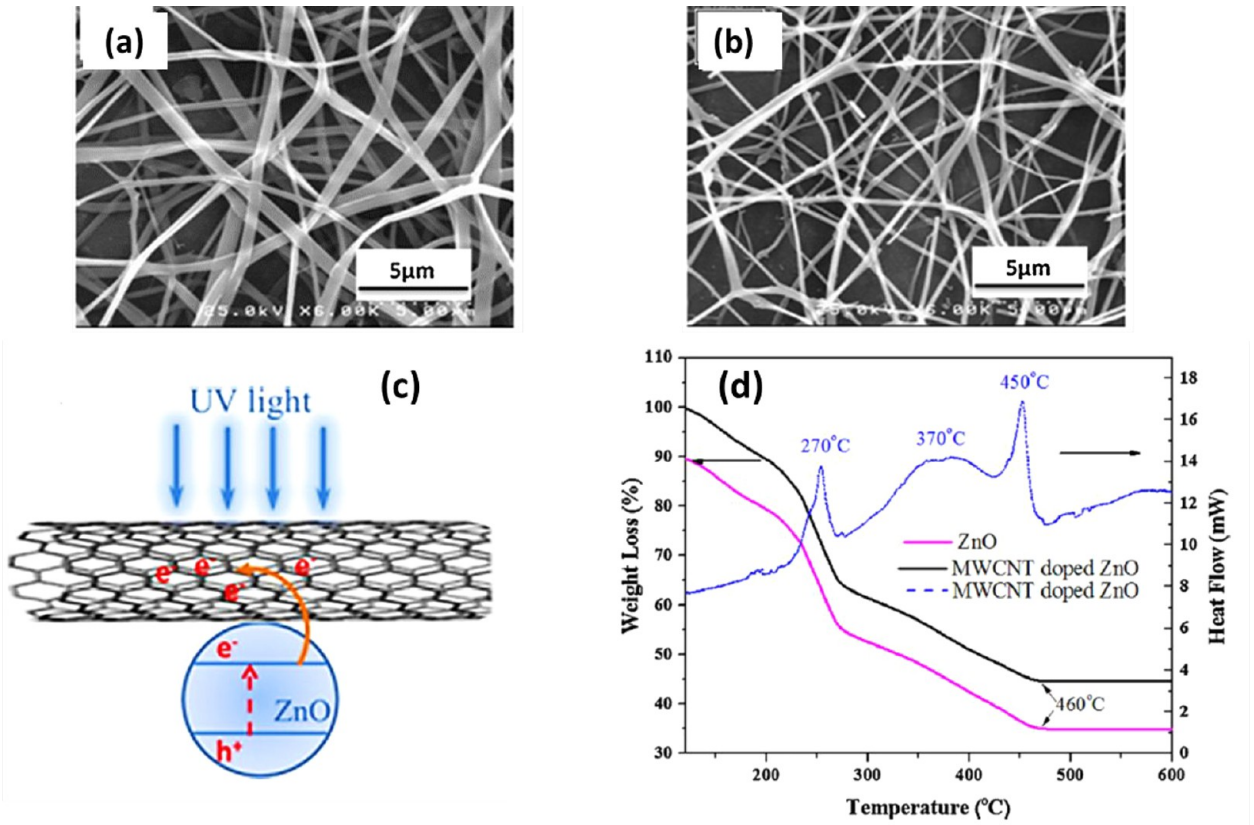

Figure 8. FESEM images of ZnO nanofibers (a) before calcination and (b) after calcination. (c) Mechanism of electron−hole separation under UV light illumination of the ZnO−MWCNT nanofibers. (d) TGA−DTA of ZnO and ZnO-MWCNT nanofibers. Reprinted with permission from ref 25. Copyright 2012 Elsevier Science Ltd.

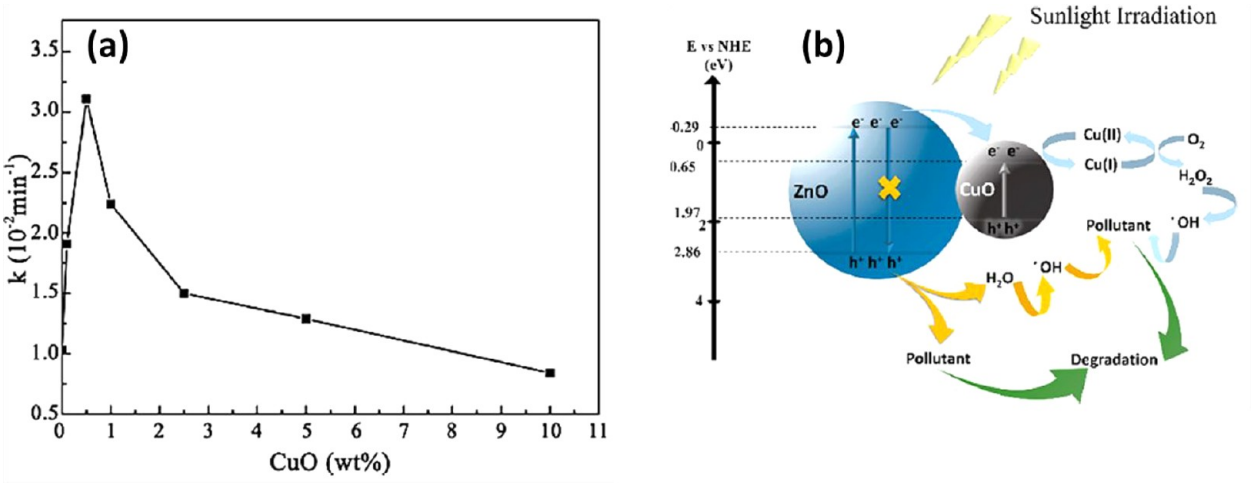

Figure 9. (a) Rate constants for photocatalytic degradation of MB over various ZnO/x wt % CuO (x = 50, 10, 5, 2.5, 1, 0.5, 0.1, and 0) nanofibers photocatalysts under simulated solar light. (b) Schematic for the charge carrier generation on the ZnO/0.5 wt % CuO electrospun nanofibers and the related degradation of MB as a model of organic pollutant. Reprinted with permission from ref 26. Copyright 2017 American Chemical Society.

retardation of their recombination. The photogenerated electrons on the ZnO CB transfer to the CuO CB and convert Cu^{2+} to Cu^{+}; then, H_2O_2 and $^{\bullet}OH$ are produced via Cu^{+} to Cu^{2+} reduction. On the other side, the holes on the ZnO VB can oxidize water to produce $^{\bullet}OH$, and then the generated $^{\bullet}OH$ attacks MB directly, leading to its photodegradation. MB degradation can also occur via produced $^{\bullet}OH$ species through H_2O_2 conversion.

Another method for synthesizing multicomponent composites is to produce one component by electrospinning and then grow the other components with another chemical method. Zhou et al. fabricated TiO_2 nanofibers by annealing tetrabutyl titanate ($Ti(OC_4H_9)_4$)/PVP electrospun nanofibers and then grew g-C_3N_4 on the nanofibers.[27] Evaporation of urea beneath the electrospun TiO_2 nanofibers at high temperature led to its thermal vapor condensation and deposition of g-C_3N_4 on nanofibers. Different amounts of urea, including 1, 2, and 3 g,

https://doi.org/10.1021/acsomega.2c05624
ACS Omega 2022, 7, 45867−45881

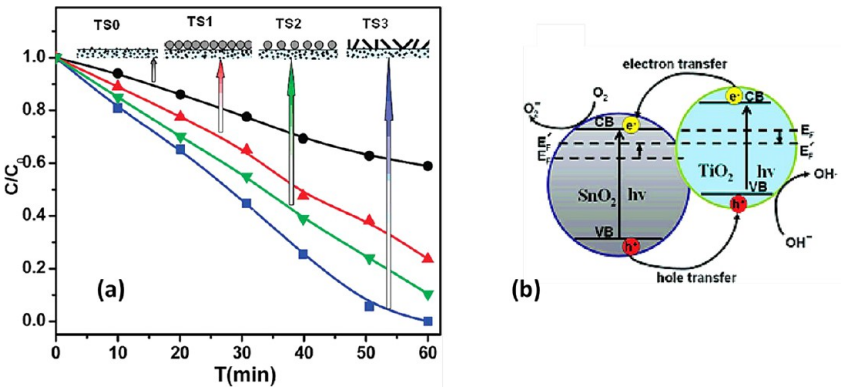

Figure 10. (a) Variation of C/C_0 ratios with time for photocatalytic degradation of RB over different TiO_2/SnO_2 samples. (b) Schematic of electron−hole pair generation and separation in the SnO_2/TiO_2 heterostructure. Reprinted with permission from ref 28. Copyright 2009 American Chemical Society.

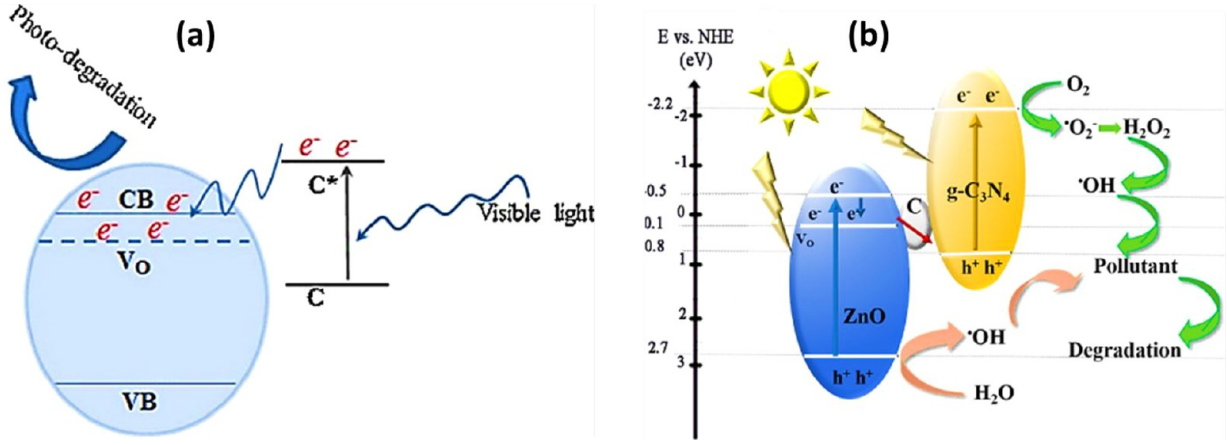

Figure 11. (a) Role of carbon species as a photosensitizer under visible light illumination in ZnO−carbon nanofibers. Reprinted with permission from ref 29. Copyright 2013 Elsevier Science Ltd. (b) Schematic generation of electron−hole pairs and reactive oxygen species during photocatalytic process over the $ZnO/C/g\text{-}C_3N_4$ nanofibers for the pollutant degradation. Reprinted with permission from ref 30. Copyright 2021 Elsevier Science Ltd.

were applied to prepare $g\text{-}C_3N_4/TiO_2$-1, $g\text{-}C_3N_4/TiO_2$-2, and $g\text{-}C_3N_4/TiO_2$-3 samples, respectively. The best RhB photocatalytic degradation was for $g\text{-}C_3N_4/TiO_2$-2 with a suitable specific surface area and proper density of $g\text{-}C_3N_4$ compared to the others.

Wang et al. prepared pristine TiO_2 nanofibers and then grew different SnO_2 nanostructures using the hydrothermal method.[28] They changed the precursor solution and applied temperature for heat treatment. In Figure 10a, TS0, TS1, TS2, and TS3 denote pristine TiO_2, high-density SnO_2 nanoparticles on TiO_2, low-density SnO_2 nanoparticles on TiO_2, and SnO_2 nanorods on TiO_2, respectively. The higher RB photocatalytic degradation of TS3 was attributed to the higher crystallinity and fewer defect states of SnO_2 nanorods. The mechanism of photocatalytic degradation on the TiO_2/SnO_2 samples is shown in Figure 10b, representing a type II heterostructure, as explained in Figure 4a.

By annealing the polymer and semiconductor precursor nanofibers in an oxygen-deficient atmosphere (N_2 or Ar environment) in which the oxidation and elimination of carbon materials are incomplete, amorphous carbon species formation and semiconductor crystallization occur simultaneously.[29] Figure 11a exhibits the role of this carbon species as a photosensitizer to inject photogenerated electrons to the CB of ZnO during light illumination. In addition, the formation of ZnO in an oxygen-deficient atmosphere results in oxygen vacancies as defect states in its band gap. These defect states promote the separation of the electron−hole pairs and provide band-gap tuning for light absorption. Therefore, the photocatalyst has a charge transfer mechanism as described earlier in Figure 4d and 4f.

In another study, to prepare $ZnO/carbon/(x\ wt\ \%)\ g\text{-}C_3N_4$ nanofibers, different amounts of $g\text{-}C_3N_4$ nanosheets were mixed with PVA and zinc acetate dihydrate as a precursor of the electrospinning technique and then annealed at 460 °C under a N_2 atmosphere.[30] As shown in Figure 11b, the Z-scheme charge transfer mechanism governs photocatalytic degradation in $ZnO/C/g\text{-}C_3N_4$ samples. Photogenerated electrons on ZnO CB recombine with $g\text{-}C_3N_4$ VB holes, and the carbon species can act as an electron channel for efficient recombination. Also, the accumulated electrons in the $g\text{-}C_3N_4$ CB and holes in the ZnO VB with suitable redox potentials are responsible for generating charge carriers to perform photodegradation. The following equations (eqs 5−11) were proposed for the degradation of MB on the $ZnO/carbon/g\text{-}C_3N_4$ nanocomposite photocatalyst

$$ZnO/C/g\text{-}C_3N_4 + h\nu \rightarrow e^-(CB_{g\text{-}C3N4}) + h^+(VB_{ZnO}) \quad (5)$$

$$H_2O + h^+ \rightarrow H^+ + {}^\bullet OH \quad (6)$$

https://doi.org/10.1021/acsomega.2c05624
ACS Omega 2022, 7, 45867−45881

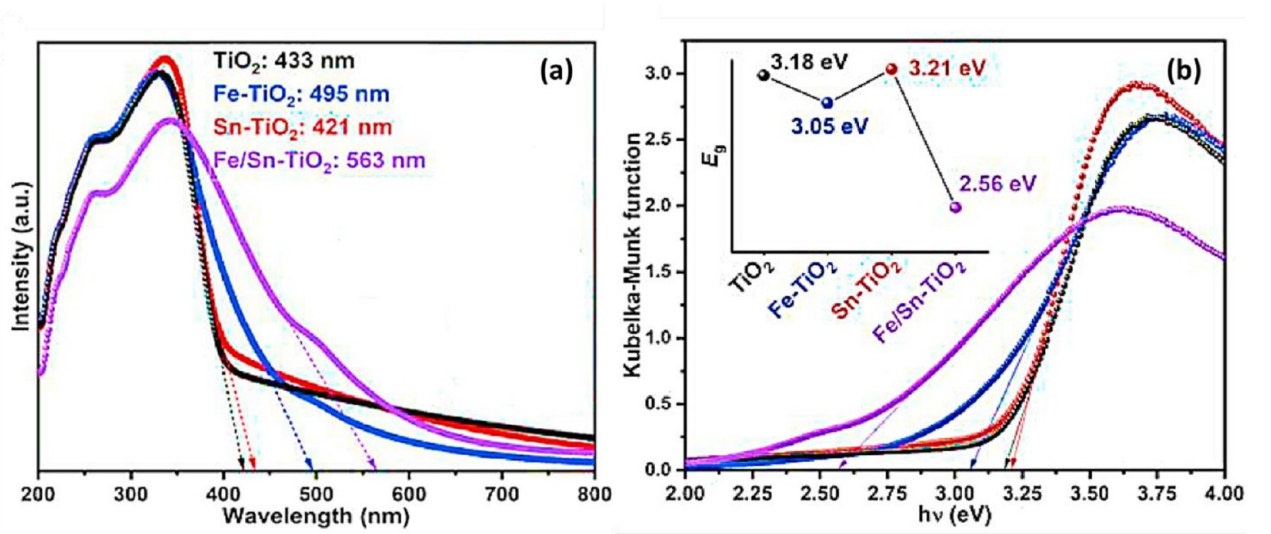

Figure 12. (a) UV−vis absorption spectra of TiO_2, Fe-doped TiO_2 (Fe−TiO_2), Sn-doped TiO_2 (Sn−TiO_2), and Fe/Sn-codoped TiO_2 (Fe/Sn−TiO_2) nanofibers. (b) Corresponding Tauc plots and band-gap values. Reprinted with permission from ref 31. Copyright 2021 Elsevier Science Ltd.

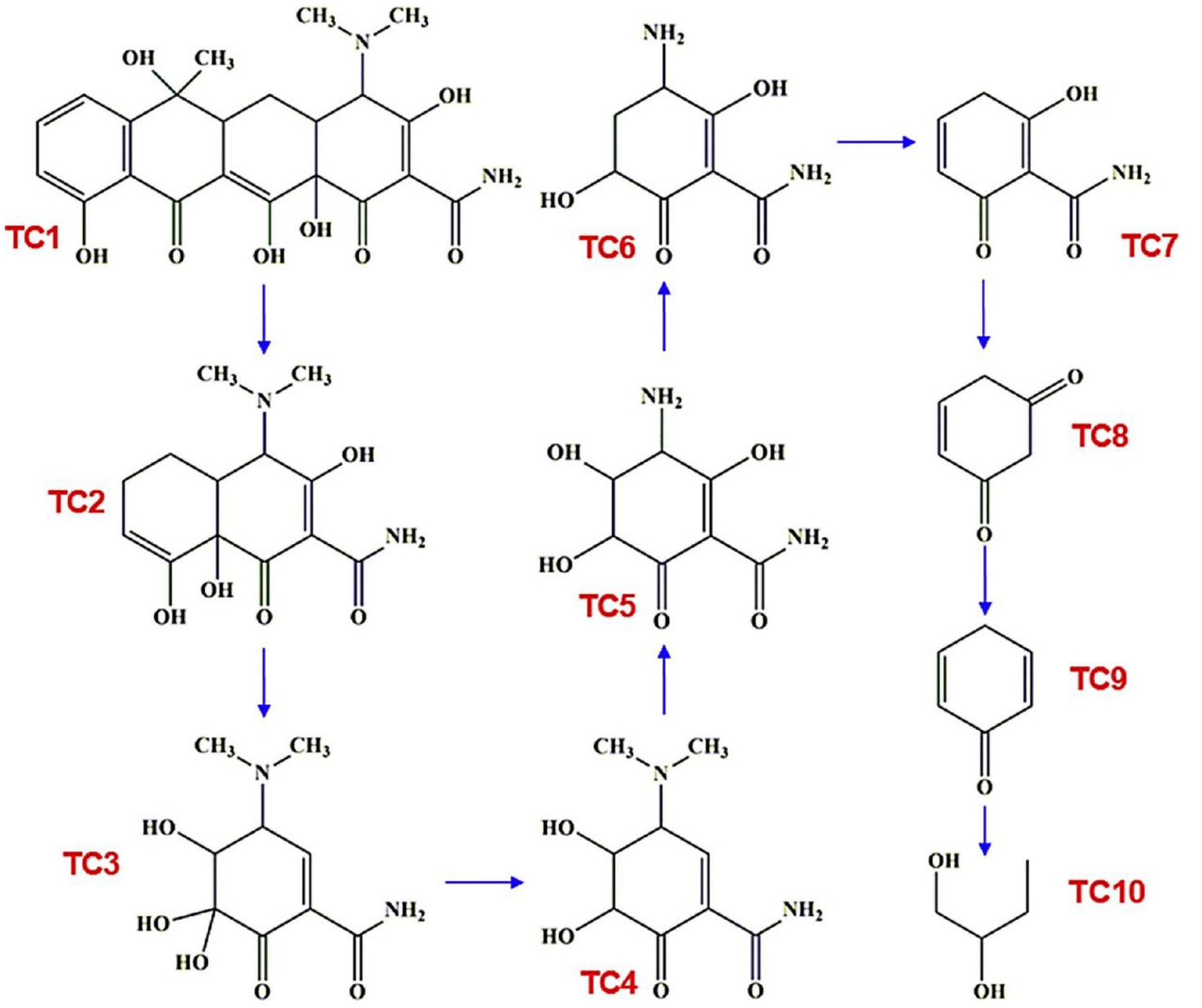

Figure 13. Pathway for TC photodegradation over Fe/Sn-codoped TiO_2 nanofibers. Reprinted with permission from ref 31. Copyright 2021 Elsevier Science Ltd.

https://doi.org/10.1021/acsomega.2c05624
ACS Omega 2022, 7, 45867−45881

$$O_2 + e^- \rightarrow O_2^{-\bullet} \quad (7)$$

$$O_2^{-\bullet} + 2H^+ + e^- \rightarrow H_2O_2 \quad (8)$$

$$H_2O_2 + H^+ + e^- \rightarrow {}^{\bullet}OH + H_2O \quad (9)$$

$${}^{\bullet}OH + MB \rightarrow \text{intermediates} \rightarrow CO_2 + H_2O + \text{harmless chemicals} \quad (10)$$

$$O_2^{-\bullet} + MB \rightarrow \text{intermediates} \rightarrow CO_2 + H_2O + \text{harmless chemicals} \quad (11)$$

Briefly, in this mechanism, the accumulated photogenerated electrons on the g-C_3N_4 CB reduce O_2 to $O_2^{-\bullet}$; then, $O_2^{-\bullet}$ converts to H_2O_2 to generate the hydroxyl radical ($^{\bullet}OH$) as a powerful oxidizing agent for organic compound oxidation. At the same time, the accumulated photogenerated holes on the ZnO react with water to produce $^{\bullet}OH$ for MB degradation.

Doping of a metal and nonmetal induces new energy states into the forbidden band gap of the wide-band-gap semiconductor, which can cause the absorption of large fractions of the illuminated sunlight.[2] Iron and tin were utilized as dopants for TiO_2 electrospun nanofibers and applied for tetracycline (TC) photodegradation.[31] Figure 12a shows the UV−vis absorption spectra of TiO_2, Fe-doped TiO_2 (Fe−TiO_2), Sn-doped TiO_2 (Sn−TiO_2), and Fe/Sn-codoped TiO_2 (Fe/Sn−TiO_2) samples. Their related absorption edges change from 433 to 563 nm. Codoping induces a broader light absorption range, which is favorable for a photocatalytic process under solar illumination. The band-gap values of the photocatalysts were calculated using the Kubelka−Munk method, and the Tauc plot is shown in Figure 12b. The results confirm band-gap narrowing through doping, and the codoping sample with the highest photocatalytic activity possesses the lowest band-gap value. The photodegradation enhancement via doping was attributed to forming the new energy levels of dopants below the CB of TiO_2, which can efficiently trap photogenerated electrons and suppress hole recombination. Liquid chromatography-tandem mass spectrometry (LC-MS) was utilized to study the reaction intermediates during the TC photodegradation, and the possible pathway is illustrated in Figure 13. It approves the efficient TC photodecomposition to a lower molecular weight compound (TC10) and subsequent conversion to CO_2 and H_2O.

4.2.2. Electrospun Nanofibers Mat as a Substrate. The second strategy applies the electrospun polymer nanofibers as a carrier for photocatalyst immobilization (see Figure 5, approach 2). For conducting this approach, there are two different methods. In method 1, the photocatalyst is mixed with a polymer solution as an electrospinnable precursor, and in method 2, electrospun nanofibers are utilized as a substrate for growing the photocatalyst materials. The following section presents results of applying these two methods to prepare electrospinning-based photocatalysts separately.

In method 1, PVA with an average molecular weight of M_w = 66 000, TiO_2 nanopowder with a particle size of 18 nm, and distilled water were mixed as a spinnable solution.[32] Uniform nanofibers with no beads were formed at a 13% PVA solution. The effect of different amounts of TiO_2 on the morphological changes of PVA/TiO_2 nanofibers demonstrated that the viscosities of the electrospinning solutions are inversely related to TiO_2 amounts. Higher quantities of TiO_2 reduced the viscosity; thus, thinner nanofibers with a higher specific surface area formed. As PVA is water soluble, thermal treatment at 155 °C for 10 min was performed to form a suitable membrane for photocatalytic water treatment, which was not dissolved in the aqueous moiety.

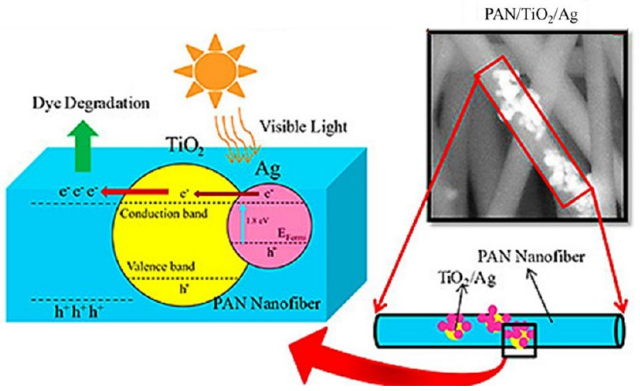

Figure 14. Mechanism of dye degradation on PAN/TiO_2/Ag nanofibers and its corresponding SEM image. Reprinted with permission from ref 33. Copyright 2021 American Chemical Society.

To prepare a water-insoluble membrane, PAN, *N*,*N*-dimethylformamide (DMF), TiO_2, and $AgNO_3$ were mixed for loading in an electrospinning syringe to prepare the PAN/TiO_2/Ag nanofiber.[33] As depicted in the SEM image of Figure 14, TiO_2/Ag nanoparticles are deposited on PAN nanofibers. The photocatalytic reaction mechanism was investigated, and the schematic of the photogenerated charge carriers' generation is illustrated in Figure 14. The enhanced degradation of methylene blue and methylene orange is attributed to the role of Ag nanoparticles as a photosensitizer. The photogenerated electrons from the Ag surface inject into the TiO_2 CB to perform photodegradation of the dyes.

In the other study, TiO_2 nanoparticles were mixed with PAN solution to fabricate the PAN/TiO_2 membrane photocatalyst.[34] Due to the piezoelectric property of PAN nanofibers, the photodegradation of rhodamine B (RhB) under sonication conditions exhibited a 2.5 times enhancement in the rate compared to conventional conditions. The piezoelectric fields in PAN promoted the separation of the photogenerated electron−hole pairs in TiO_2 and improved the photocatalytic efficiency. In another report, $BiOBr_xI_{1-x}$ photocatalysts were anchored on flexible electrospun PAN nanofiber mats.[20] By changing the x values, the band gaps of the samples were varied: 2.95, 2.23, 2.07, 1.85, and 1.79 eV for x = 1.0, 0.8, 0.5, 0.2, and 0.0, respectively. The results showed that $BiOBr_{0.5}I_{0.5}$@PAN demonstrated a better photodegradation efficiency for the methyl orange (MO) and bisphenol A (BPA) photodegradation processes. Although the light absorption range expanded by increasing x values, the appropriate redox potentials of the charge carriers in the $BiOBr_{0.5}I_{0.5}$@PAN are responsible for its higher photodegradation efficiency. Figure 15a shows the SEM image of the optimized $BiOBr_{0.5}I_{0.5}$@PAN nanofiber photocatalyst. Concerning the floating status of the optimized $BiOBr_{0.5}I_{0.5}$ anchored on electrospun PAN, it has been reported that during the photocatalytic process the recyclability of the sample can be obtained as shown in Figure 15b.

Liu et al. studied various electrospun PVDF, TiO_2, and SiO_2 nanofiber solutions on modified conductive carbon fiber cloth (CFC).[35] They compared the photodegradation of different anionic (such as MO) and cationic (such as RhB and MB) dyes

https://doi.org/10.1021/acsomega.2c05624
ACS Omega 2022, 7, 45867−45881

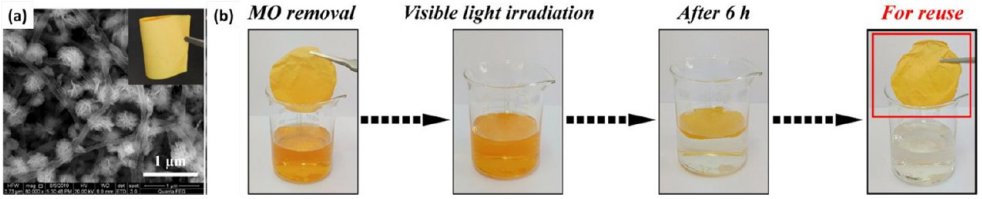

Figure 15. (a) SEM image of $BiOBr_{0.5}I_{0.5}$ anchored on electrospun PAN nanofiber. (b) Recyclability and floating status of $BiOBr_{0.5}I_{0.5}$@PAN nanocomposite with time during the photocatalysis process. Reprinted with permission from ref 20. Copyright 2022 Elsevier Science Ltd.

under simulated sunlight irradiation. The results demonstrated removal rates of 99.17%, 99.69%, and 38.76% for RhB, MB, and MO under similar conditions, respectively. The selective removal of cationic dyes was due to the negative charge on the electrospun PVDF/TiO_2/SiO_2 photocatalyst.

Mixing photocatalysts with the polymer in method 1 may have a drawback of limited access to the photocatalyst because it is embedded in the polymer matrix. To solve this issue, various PVDF:PVP weight ratios (18:0, 12:6, 9:9, and 6:12) and 4 wt % TiO_2 nanoparticles were utilized for electrospinning.[36] The PVP part of the sample can be removed by immersing the nanofibers in water, and a porous PVDF mat with TiO_2 was formed. This nonporous mat was rough and had an increased specific surface area, which is favorable for the photocatalytic degradation of bisphenol A and MB. In addition, PVP dissolving during the process could facilitate the accessibility to TiO_2 photocatalyst.

In method 2, electrospun polymer nanofibers are utilize as a platform for synthesizing photocatalysts.[37] Electrospun PAN nanofibers were dip coated in triethylamine and zinc acetate as a seed solution for ZnO.[38] Then, growth of the ZnO nanorod occurred by immersing it in a mixed solution of zinc nitrate

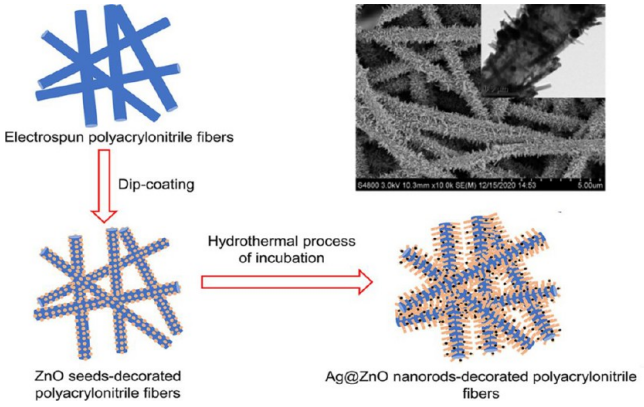

Figure 16. Schematic of the Ag@ZnO nanorods decorated on the PAN membrane; (inset) related SEM image. Reprinted with permission from ref 38. Copyright 2021 Elsevier Science Ltd.

hexahydrate and hexamethylenetetramine. Besides, a silver nitrate solution was used to deposit Ag nanoparticles on the ZnO nanorods. Figure 16 shows the schematic of the preparation of Ag@ZnO nanorods on the PAN membrane, and the inset shows the related SEM image. In the other work, polyurethane electrospun nanofibers were used to grow ZnO nanorods to study the photodegradation of methylene blue.[39] The surface of the pristine polyurethane nanofibers was functionalized with polydopamine to induce proper attachment of ZnO nanorods on the electrospun nanofibers. The chemical bond between ZnO and polyurethane can solve the leaching problem of photocatalysts during the process. Moreover, the catechol group of polydopamine acted as a photogenerated electron trap and hindered electron−hole recombination.[39]

To summarize, we provided an overview of the electrospinning-based photocatalyst fabrication (see Figure 5) and reviewed recently published articles. In approach 1, the electrospun polymer nanofibers are applied as a sacrificing template to form a 1D semiconductor photocatalyst. In this method, pure and hybrid nanocomposite photocatalysts can be provided. The major challenge of this method is to select a suitable precursor for semiconductor formation and an appropriate annealing temperature for both photocatalyst crystallization and polymer template elimination. Although this method is reliable and versatile for producing several pure and hybrid photocatalysts, the low production rate with lab-scale electrospinning machines encourages the utilization of multinozzle or nozzleless electrospinning machines to upgrade its industrial production. Another challenge is to recover the used photocatalysts from the treated water for reusability assessment.

Approach 2 utilizes the polymer carrier as the backbone for photocatalyst formation. Although the electrospun mat's flexibility is helpful for practical applications, its wrinkling and folding upon exposure to semiconductor growth solution is the primary concern. Moreover, the selection of the polymer should be such that it does not dissolve in the growth solution. Regarding these challenges, physical methods for depositing photocatalysts are more favorable. An appropriate chemical anchoring between the photocatalyst and the electrospun membrane should be considered to provide reliable recovery and reusability of the photocatalyst. Furthermore, the leaching of photocatalysts into the treated water should be tested to obtain the proper stability. Moreover, the chemical stability of the polymer nanofibers should be considered during the reaction between the charge carriers and/or the ROS species with the polymer surface. However, the positive aspect of this method is that the highly porous nature of the electrospun polymeric mat can provide synergistic adsorption and photocatalytic degradation for efficient wastewater treatment.

5. CONCLUSIONS AND FUTURE DIRECTIONS

In recent years, the electrospinning process has been of great interest to researchers because of its ability to synthesize a wide range of 1D nanostructures containing polymers, organic and inorganic materials, and composites. Simplicity, low cost, and industrial production capability are other advantages of this method. Furthermore, electrospun nanofibers are nonwoven mats, providing a high surface area for adsorption and filtration applications in wastewater treatment. Combining these advantages with semiconductor photocatalyst materials that are able to decompose organic pollutants without causing secondary pollution will strengthen the electrospun nanofibers applications.

https://doi.org/10.1021/acsomega.2c05624
ACS Omega 2022, 7, 45867−45881

In this review, the relevance of the electrospinning method in photocatalytic applications was thoroughly investigated and described according to recently published articles. Overall, there are mainly two strategies for applying electrospun nanofibers for photocatalytic degradation of water pollutants. Despite the remarkable progress in this field, there are some challenges and limitations. In the first strategy, although the fabrication of a 1D semiconductor photocatalyst through annealing the polymer and saline precursors is a simple method, a low production yield is still one of the significant disadvantages that limits its application. Moreover, filtration or centrifugation may be required to separate the photocatalysts from the treated water, restricting their industrial application and effects on reusability.

Post-treatment of the polymeric nanofibers' membrane by photocatalyst materials with self-supporting properties is focused on the second strategy, which has recently received more attention. In this approach, the photocatalyst is applied as a floating membrane; therefore, the energy-intensive separation process is not required, which is appealing for industrial use. Here, the primary concern is the flexibility and poor mechanical strength of the nanofibers for the growth and deposition of photocatalysts. Also, the uniformity of the photocatalyst on the nanofiber membrane may vary in different samples due to the lack of accurate control of synthesis parameters, which affects repeatability. Determining the exact amount of photocatalyst deposited on the membrane is another challenge, making it difficult to compare the yield of different samples. Moreover, photocatalyst leaching due to the improper attachment to the nanofibers should be investigated by reusability and repeatability tests. The other issue is the stability concern of the polymeric substrate during successive usage of nanofibers membrane.

Considering the strengths and shortcomings discussed in this review, potential directions for future research are listed below.

- Although the parameters of the electrospinning process have been formulated, there are few quantitative studies on the relationship between experimental research and mathematical parameters, and most of the works have been qualitative reports.
- Thus far, producing nanofibers with diameters below 50 nm, which create a larger surface area and improve water purification, has not been successful. Therefore, further research could be conducted to achieve thinner nanofibers by tuning the electrospinning parameters.
- At the mass-production level, large amounts of evaporated organic solvents enter the environment and make electrospinning not environmentally friendly. To overcome this dilemma, melt electrospinning or installation of a solvent recovery system is recommended.
- The chemical functionalization of electrospun nanofibers can induce a chemical bond between them and the photocatalysts, hindering the detachment and unwanted release of the photocatalyst.
- Visible light active photocatalysts are encouraged due to the use of solar irradiation as a cheap, abundant, and clean light source. This issue has recently received much attention because of extensive fossil fuel use causing environmental pollution.
- Emerging aquatic pollutants, including personal care products, pharmaceuticals, and endocrine-disrupting chemicals, have entered into the surface water through human excretion. All of these products are of concern for humans for effective wastewater treatment. The photocatalytic process can remove some of them, while the ineffectiveness of conventional treatment is proved. Therefore, addressing this issue is essential and valuable beyond removing organic dyes.
- Utilizing the nozzleless electrospinning technique can facilitate the issue of the low product yield of electrospun photocatalysts.
- As explained by eq 4, the photocatalytic process is suitable for low pollutant concentrations. Fabricating electrospinning-based photocatalysts with high adsorption capacity can boost wastewater treatment due to the adsorption/photocatalysis synergy.
- Combining the polymeric piezoelectric membrane and the piezophotocatalyst enhances the charge carrier separation and the photodegradation efficiency. Addressing these combined materials can lead to the fabrication of multifunctional membranes for air and water purification.

AUTHOR INFORMATION

Corresponding Authors

Morasae Samadi − *Department of Physical Chemistry and Nanochemistry, Faculty of Chemistry, Alzahra University, Tehran 19938-93973, Iran;* orcid.org/0000-0003-0216-1636; Email: m.samadi@alzahra.ac.ir

Alireza Zaker Moshfegh − *Department of Physics, Sharif University of Technology, Tehran 11555-9161, Iran; Institute for Nanoscience and Nanotechnology, Sharif University of Technology, Tehran 14588-89694, Iran;* orcid.org/0000-0002-8770-1410; Email: moshfegh@sharif.edu

Complete contact information is available at: https://pubs.acs.org/10.1021/acsomega.2c05624

Notes

The authors declare no competing financial interest.

ACKNOWLEDGMENTS

The authors thank the Research Council of the Sharif University of Technology and Alzahra University for supporting this project. A.Z.M. thanks INSF through the Chair of Surface/Interface Program (940009) for financial assistance.

REFERENCES

(1) Baaloudj, O.; Assadi, I.; Nasrallah, N.; El Jery, A.; Khezami, L.; Assadi, A. A. Simultaneous removal of antibiotics and inactivation of antibiotic-resistant bacteria by photocatalysis: A review. *J. Water Process. Eng.* **2021**, *42*, 102089−102100. Tkaczyk, A.; Mitrowska, K.; Posyniak, A. Synthetic organic dyes as contaminants of the aquatic environment and their implications for ecosystems: A review. *Sci. Total Environ.* **2020**, *717*, 137222−137241.

(2) Samadi, M.; Zirak, M.; Naseri, A.; Khorashadizade, E.; Moshfegh, A. Z. Recent progress on doped ZnO nanostructures for visible-light photocatalysis. *Thin Solid Films* **2016**, *605*, 2−19.

(3) Rahman, A.; Jennings, J. R.; Tan, A. L.; Khan, M. M. Molybdenum Disulfide-Based Nanomaterials for Visible-Light-Induced Photocatalysis. *ACS Omega* **2022**, *7* (26), 22089−22110.

(4) Samadi, M.; Zirak, M.; Naseri, A.; Kheirabadi, M.; Ebrahimi, M.; Moshfegh, A. Z. Design and tailoring of one-dimensional ZnO nanomaterials for photocatalytic degradation of organic dyes: a review. *Res. Chem. Intermed.* **2019**, *45* (4), 2197−2254.

(5) Choi, S. K.; Kim, S.; Lim, S. K.; Park, H. Photocatalytic Comparison of TiO_2 Nanoparticles and Electrospun TiO2 Nanofibers: Effects of Mesoporosity and Interparticle Charge Transfer. *J. Phys. Chem. C* **2010**, *114* (39), 16475−16480. Regonini, D.; Teloeken, A. C.; Alves, A. K.; Berutti, F. A.; Gajda-Schrantz, K.; Bergmann, C. P.; Graule,

T.; Clemens, F. Electrospun TiO_2 Fiber Composite Photoelectrodes for Water Splitting. *ACS Appl. Mater. Interfaces* **2013**, *5* (22), 11747−11755.
(6) Li, D.; Xia, Y. Electrospinning of nanofibers: Reinventing the wheel? *Adv. Mater.* **2004**, *16* (14), 1151−1170. Hosseini, S. A.; Daneshvar e Asl, S.; Vossoughi, M.; Simchi, A.; Sadrzadeh, M. Green Electrospun Membranes Based on Chitosan/Amino-Functionalized Nanoclay Composite Fibers for Cationic Dye Removal: Synthesis and Kinetic Studies. *ACS Omega* **2021**, *6* (16), 10816−10827. Jamil, T.; Munir, S.; Wali, Q.; Shah, G. J.; Khan, M. E.; Jose, R. Water Purification through a Novel Electrospun Carbon Nanofiber Membrane. *ACS Omega* **2021**, *6* (50), 34744−34751.
(7) Xue, J.; Wu, T.; Dai, Y.; Xia, Y. Electrospinning and Electrospun Nanofibers: Methods, Materials, and Applications. *Chem. Rev.* **2019**, *119* (8), 5298−5415.
(8) Liao, Y.; Loh, C.-H.; Tian, M.; Wang, R.; Fane, A. G. Progress in electrospun polymeric nanofibrous membranes for water treatment: Fabrication, modification and applications. *Prog. Polym. Sci.* **2018**, *77*, 69−94.
(9) Shi, Y.; Huang, J.; Zeng, G.; Cheng, W.; Hu, J. Photocatalytic membrane in water purification: is it stepping closer to be driven by visible light? *J. Membr. Sci.* **2019**, *584*, 364−392. Chabalala, M. B.; Gumbi, N. N.; Mamba, B. B.; Al-Abri, M. Z.; Nxumalo, E. N. Photocatalytic Nanofiber Membranes for the Degradation of Micropollutants and Their Antimicrobial Activity: Recent Advances and Future Prospects. *Membranes* **2021**, *11* (9), 678−710. Nasir, A. M.; Awang, N.; Jaafar, J.; Ismail, A. F.; Othman, M. H. D.; A. Rahman, M.; Aziz, F.; Mat Yajid, M. A. Recent progress on fabrication and application of electrospun nanofibrous photocatalytic membranes for wastewater treatment: A review. *J. Water Process. Eng.* **2021**, *40*, 101878−101900. Li, N.; Ma, J.; Zhang, Y.; Zhang, L.; Jiao, T. Recent Developments in Functional Nanocomposite Photocatalysts for Wastewater Treatment: A Review. *Adv. Sustainable Syst.* **2022**, *6* (7), 2200106−2200119.
(10) Lu, N.; Zhang, M.; Jing, X.; Zhang, P.; Zhu, Y.; Zhang, Z.Electrospun Semiconductor-Based Nano-Heterostructures for Photocatalytic Energy Conversion and Environmental Remediation: Opportunities and Challenges.*Energy Environ. Mater.***2022** DOI: 10.1002/eem2.12338. Xu, F.; Tan, H.; Fan, J.; Cheng, B.; Yu, J.; Xu, J. Electrospun TiO_2-Based Photocatalysts. *Sol. RRL* **2021**, *5* (6), 2000571−2000599.
(11) Asgari, S.; Mohammadi Ziarani, G.; Badiei, A.; Ajalloueian, F.; Vasseghian, Y. Electrospun composite nanofibers as novel high-performance and visible-light photocatalysts for removal of environmental pollutants: A review. *Environ. Res.* **2022**, *215*, 114296−1143319.
(12) Liu, Y.; Wang, C.*Advanced nanofibrous materials manufacture technology based on electrospinning*; CRC Press, 2019.
(13) Taylor, G. I. Electrically driven jets. *Proc. R. Soc. London, Ser. A* **1969**, *313* (1515), 453−475.
(14) Ramakrishna, S.*An introduction to electrospinning and nanofibers*; World Scientific, 2005. Bhardwaj, N.; Kundu, S. C. Electrospinning: A fascinating fiber fabrication technique. *Biotechnol. Adv.* **2010**, *28* (3), 325−347.
(15) Ghosal, K.; Chandra, A.; G., P.; S., S.; Roy, S.; Agatemor, C.; Thomas, S.; Provaznik, I. Electrospinning over Solvent Casting: Tuning of Mechanical Properties of Membranes. *Sci. Rep.* **2018**, *8* (1), 5058−5067.
(16) Naseri, A.; Samadi, M.; Pourjavadi, A.; Moshfegh, A. Z.; Ramakrishna, S. Graphitic carbon nitride ($g\text{-}C_3N_4$)-based photocatalysts for solar hydrogen generation: recent advances and future development directions. *J. Mater. Chem. A* **2017**, *5* (45), 23406−23433.
(17) Turchi, C. S.; Ollis, D. F. Photocatalytic degradation of organic water contaminants: Mechanisms involving hydroxyl radical attack. *J. Catal.* **1990**, *122* (1), 178−192.
(18) Le, T. T.; Lee, M.; Chae, K. H.; Moon, G.-H.; Kim, S. H. Control of copper element in mesoporous iron oxide photocatalysts towards UV light-assisted superfast mineralization of isopropyl alcohol with peroxydisulfate. *Chem. Eng. J.* **2023**, *451*, 139048−139058.
(19) Lan, M.; Zheng, N.; Dong, X.; Wang, Y.; Wu, J.; Ren, X.; Gao, J. Application of flexible PAN/BiOBr-Cl microfibers as self-supporting and highly active photocatalysts for nitrogen fixation and dye degradation. *Appl. Surf. Sci.* **2022**, *575*, 151743−1517751. Wang, Q.; Ji, S.; Li, S.; Zhou, X.; Yin, J.; Liu, P.; Shi, W.; Wu, M.; Shen, L. Electrospinning visible light response Bi_2MoO_6/Ag_3PO_4 composite photocatalytic nanofibers with enhanced photocatalytic and antibacterial activity. *Appl. Surf. Sci.* **2021**, *569*, 150955−150968.
(20) Liu, S.; Liang, P.; Liu, J.; Xin, J.; Li, X.; Shao, C.; Li, X.; Liu, Y. Anchoring bismuth oxybromo-iodide solid solutions on flexible electrospun polyacrylonitrile nanofiber mats for floating photocatalysis. *J. Colloid Interface Sci.* **2022**, *608*, 3178−3191.
(21) Ji, W.; Wang, X.; Ding, T.; Chakir, S.; Xu, Y.; Huang, X.; Wang, H. Electrospinning preparation of nylon-6@UiO-66-NH_2 fiber membrane for selective adsorption enhanced photocatalysis reduction of Cr(VI) in water. *Chem. Eng. J.* **2023**, *451*, 138973−138983.
(22) Lan, M.; Wang, M.; Zheng, N.; Dong, X.; Wang, Y.; Gao, J. Hierarchical polyurethane/RGO/BiOI fiber composite as flexible, self-supporting and recyclable photocatalysts for RhB degradation under visible light. *J. Ind. Eng. Chem.* **2022**, *108*, 109−117.
(23) Dai, X.; Li, X.; Zhang, M.; Xie, J.; Wang, X. Zeolitic Imidazole Framework/Graphene Oxide Hybrid Functionalized Poly(lactic acid) Electrospun Membranes: A Promising Environmentally Friendly Water Treatment Material. *ACS Omega* **2018**, 3 (6), 6860−6866.
(24) Ligon, C.; Latimer, K.; Hood, Z. D.; Pitigala, S.; Gilroy, K. D.; Senevirathne, K. Electrospun metal and metal alloy decorated TiO_2 nanofiber photocatalysts for hydrogen generation. *RSC Adv.* **2018**, *8* (57), 32865−32876. Sarngan, P. P.; Lakshmanan, A.; Dutta, A.; Sarkar, D. Understanding the effect of polymer concentrations on the phase formation and activity of electrospun nanofibrous photocatalyst. *Colloids Surf., A* **2022**, *654*, 130182−130193.
(25) Samadi, M.; Shivaee, H. A.; Zanetti, M.; Pourjavadi, A.; Moshfegh, A. Visible light photocatalytic activity of novel MWCNT-doped ZnO electrospun nanofibers. *J. Mol. Catal. A: Chem.* **2012**, *359*, 42−48.
(26) Naseri, A.; Samadi, M.; Mahmoodi, N. M.; Pourjavadi, A.; Mehdipour, H.; Moshfegh, A. Z. Tuning Composition of Electrospun ZnO/CuO Nanofibers: Toward Controllable and Efficient Solar Photocatalytic Degradation of Organic Pollutants. *J. Phys. Chem. C* **2017**, *121* (6), 3327−3338.
(27) Zhou, X.; Shao, C.; Li, X.; Wang, X.; Guo, X.; Liu, Y. Three dimensional hierarchical heterostructures of $g\text{-}C_3N_4$ nanosheets/TiO_2 nanofibers: Controllable growth via gas-solid reaction and enhanced photocatalytic activity under visible light. *J. Hazard. Mater.* **2018**, *344*, 113−122.
(28) Wang, C.; Shao, C.; Zhang, X.; Liu, Y. SnO_2 Nanostructures-TiO_2 Nanofibers Heterostructures: Controlled Fabrication and High Photocatalytic Properties. *Inorg. Chem.* **2009**, *48* (15), 7261−7268.
(29) Samadi, M.; Shivaee, H. A.; Pourjavadi, A.; Moshfegh, A. Z. Synergism of oxygen vacancy and carbonaceous species on enhanced photocatalytic activity of electrospun ZnO-carbon nanofibers: Charge carrier scavengers mechanism. *Appl. Catal., A* **2013**, *466*, 153−160.
(30) Naseri, A.; Samadi, M.; Pourjavadi, A.; Ramakrishna, S.; Moshfegh, A. Z. Enhanced photocatalytic activity of ZnO/$g\text{-}C_3N_4$ nanofibers constituting carbonaceous species under simulated sunlight for organic dye removal. *Ceram. Int.* **2021**, *47* (18), 26185−26196.
(31) Ghoreishian, S. M.; Ranjith, K. S.; Lee, H.; Park, B.; Norouzi, M.; Nikoo, S. Z.; Kim, W.-S.; Han, Y.-K.; Huh, Y. S. Tuning the phase composition of 1D TiO_2 by Fe/Sn co-doping strategy for enhanced visible-light-driven photocatalytic and photoelectrochemical performances. *J. Alloys Compd.* **2021**, *851*, 156826−156844.
(32) Yeo, J. H.; Kim, M.; Lee, H.; Cho, J.; Park, J. Facile and Novel Eco-Friendly Poly(Vinyl Alcohol) Nanofilters Using the Photocatalytic Property of Titanium Dioxide. *ACS Omega* **2020**, *5* (10), 5026−5033.
(33) Hartati, S.; Zulfi, A.; Maulida, P. Y. D.; Yudhowijoyo, A.; Dioktyanto, M.; Saputro, K. E.; Noviyanto, A.; Rochman, N. T. Synthesis of Electrospun PAN/TiO_2/Ag Nanofibers Membrane As Potential Air Filtration Media with Photocatalytic Activity. *ACS Omega* **2022**, *7* (12), 10516−10525.

https://doi.org/10.1021/acsomega.2c05624
ACS Omega 2022, 7, 45867−45881

(34) Ding, D.; Li, Z.; Yu, S.; Yang, B.; Yin, Y.; Zan, L.; Myung, N. V. Piezo-photocatalytic flexible PAN/TiO_2 composite nanofibers for environmental remediation. *Sci. Total Environ.* **2022**, *824*, 153790−153798.
(35) Liu, L.; Wang, D.; Huang, J.; Huang, Z.; Zhang, Y.; Li, L. Multicomponent Composite Membrane with Three-Phase Interface Heterostructure as Photocatalyst for Organic Dye Removal. *ACS Omega* **2022**, *7* (20), 17128−17143.
(36) Lee, C.-G.; Javed, H.; Zhang, D.; Kim, J.-H.; Westerhoff, P.; Li, Q.; Alvarez, P. J. J. Porous Electrospun Fibers Embedding TiO_2 for Adsorption and Photocatalytic Degradation of Water Pollutants. *Environ. Sci. Technol.* **2018**, *52* (7), 4285−4293.
(37) Lee, H.; Lee, H.; Ahn, S.; Kim, J. MIL-100(Fe)-Hybridized Nanofibers for Adsorption and Visible Light Photocatalytic Degradation of Water Pollutants: Experimental and DFT Approach. *ACS Omega* **2022**, *7* (24), 21145−21155.
(38) Li, B.; Kim, I. S.; Dai, S.; Sarwar, M. N.; Yang, X. Heterogeneous Ag@ZnO nanorods decorated on polyacrylonitrile fiber membrane for enhancing the photocatalytic and antibacterial properties. *Colloid Interface Sci. Commun.* **2021**, *45*, 100543−100553.
(39) Kim, J. H.; Joshi, M. K.; Lee, J.; Park, C. H.; Kim, C. S. Polydopamine-assisted immobilization of hierarchical zinc oxide nanostructures on electrospun nanofibrous membrane for photocatalysis and antimicrobial activity. *J. Colloid Interface Sci.* **2018**, *513*, 566−574.

https://doi.org/10.1021/acsomega.2c05624
ACS Omega 2022, 7, 45867−45881